JOURNAL OF ENGINEERING
AND
APPLIED SCIENCES

JEAS

Journal of Engineering and Applied Sciences, Volume 22, Number 1, June 2023, 967 - 981

Extraction of tocopherol from palm fatty acid distillate: batch equilibrium adsorption study

Kevin Tochukwu Dibia[1*], Philomena Kanwulia Igbokwe[1], Michael Chika Egwunyenga[2], Goodluck Ochuko[2]

[1]Department of Chemical Engineering, Nnamdi Azikiwe University, Faculty of Engineering Technology, Awka, Anambra State.

[2]Department of Chemical Engineering, Delta State Polytechnic Ogwashi-Uku, Faculty of Engineering Technology

[*]Corresponding Author's E-mail: tkevin.dibia@gmail.com

Abstract
Tocopherols are vital supplements with vitamin E activity necessary for inducing antioxidant and anti-inflammatory effects in vivo. This study aimed at using the concept of batch adsorption for the extraction of tocopherol from palm fatty acid distillate (PFAD). Silica gel as an adsorbent was characterized and modified to enhance its adsorptive performance. A comparative study between the untampered and the modified adsorbent samples emanating from morphological analysis, BET surface area evaluation, and FT-IR analysis demonstrated improved adsorption capabilities in the modified adsorbent sample. Adsorption equilibrium data were obtained from laboratory experiments. The adsorption performance was studied using nonlinear versions of two-parameter Langmuir and Freundlich adsorption isotherms, and three-parameter Redlich-Peterson and Koble-Corrigan adsorption isotherms. Error functions such as Sum Square of Errors (ERRSQ/SSE), Coefficient of Determination (R^2), Spearman's Correlation Coefficient (r_s), Sum of Absolute Error (EABS), Hybrid Fractional Error (HYBRID), Marquardt's Percent Standard Deviation (MPSD), and Nonlinear Chi-Square (χ^2) were the statistical metrics employed in selecting the best-fit model. By comparing values of different error functions, the Koble-Corrigan model best fits the equilibrium adsorption of tocopherol unto modified silica gel.

Keywords: Tocopherol, Palm Fatty Acid Distillate, Adsorption Isotherm Models, Error Functions, Goodness-of-fit Test.

1. Introduction

Recently, there is an emerging research interest in exploiting the utilization of plant-based by-products to develop novel high-value compounds that enhance the health-promoting properties of human beings. Undoubtedly, it is known that certain by-products from food-processing industries can be useful, marketable, or considered absolute wastes. In terms of usefulness, they could be modified, recycled or transformed into functional substances. The suitability of these by-products uniquely opens up the possibility of extracting bioactive compounds and nutrients thus creating significant opportunities for waste reduction and indirect revenue generation (Sharma et. al., 2015). One of such by-product is the palm fatty acid distillate (PFAD).

PFAD is derived from the physical refining of crude palm oil, and it is a residue from the deodorization and deacidification stages of the vegetable oil refining plant. The deodorization and deacidification stages are majorly driven by a specific type of distillation which serves as a convenient unit operation for the purification of the oil (Xu et al., 2020; Liu et al., 2008). The distillation stage takes advantage of the differences in the boiling point and performs the separation of the components in the mixture. Notably, high-temperature, high-vacuum steam distillation is the

process condition for the deodorizer as this condition is responsible for improved taste, smell, colour, and stability of the oil by stripping unwanted products (Liu et al., 2008). During the process of refining, free fatty acids (FFAs) are ejected from the oil as PFAD along with other volatile components (Xu et al., 2020). The amount of PFAD in crude palm oil is about 4% (Rakmi and Herawan, 2000) and about 3.66 tons of PFAD are generated from every 100 tons of crude palm oil (Chu et al., 2004).

Vitamin E is the generic name for a mixture of a lipid-soluble 6-hydroxychroman compound found in higher concentrations in immune cells compared to other cells in the body that exerts an antioxidant effect as its biological activity (Rakmi and Herawan, 2000; Lewis et al., 2019; Ngoc et al., 2021). It is a mixture of two distinct vitamers – tocopherols and tocotrienols – that possess general structural features: an aromatic chromanol head and a hydrophobic tridecyl (phytyl) side-chain. Tocopherols have a saturated phytyl side chain, while tocotrienols are unsaturated having three double bonds (geranyl) in their side chain. Isomers of these compounds differ in the number and configuration of their methyl substituents attached to the chromanol ring, which results in alpha-, beta-, gamma-, and delta- isomers (Serbinova et al., 1991; Wang and Quin, 1999), and these differences emphasize their role in cellular transport as antioxidants in metabolic pathways (Upadhyay and Misra, 2009). The dominant isomer in the body is alpha-tocopherol, which has three methyl groups in addition to the hydroxyl group attached to the benzene ring (Wang and Quin, 1999).

Clinical studies have demonstrated that tocopherols as vitamin E have a health-promoting effect due to their function as an antioxidant that offers synergistic protective action against free radical-mediated degenerative diseases, like cancer, ageing, and neurological diseases (Upadhyay and Misra, 2009; Aggarwal et al., 2010). Furthermore, emerging shreds of evidence from epidemiological research reveal that tocopherol is capable of preventing platelet hyper-aggression and alleviating the production of prostaglandins such as thromboxane (Rizvi et al., 2014; Khadangi and Azzi, 2019), and it also prevents the brain cells from being damaged by neuro-degradative processes (Eitenmiler and Lee, 2014). More so, tocopherols protect the polyunsaturated fatty acids (PUFAs) in the membrane from oxidation, and regulate the production of reactive oxygen species (ROS) and reactive nitrogen species (RNS), gene transcription and modulate signal transduction in many mammalian organisms (Khadangi and Azzi, 2019; Lee and Han, 2018; Lewis et al., 2019).

It is crucial to isolate beneficial phytonutrients from PFAD and supply them to the appropriate industries in a concentrated and pure form. The technique of acquiring tocopherols can be done by combining several popular processes such as neutralization, extraction, and adsorption. The neutralization process is performed to remove free fatty acids (FFAs). This process is then followed by the extraction of tocopherols from the neutralized complex matrix, using an appropriate solvent such as alcohol (Veningtia et al., 2021). The latter is a significant process that involves the use of selective adsorbents with quantum molecular-sieve characteristics to activate the extraction of the biomolecules.

In recent years, the quantitative understanding of the adsorption process has become an important aspect of process design in chemical industries. Adsorption is also regarded as a practicable separation method for purification based on the differences between the adsorption affinities of natural products for the surface of the adsorbents (Zhang et al., 2018). However, because the adsorption technique has unique features such as comparatively low cost of application – especially for well-designed sorption processes, ease of operation coupled with high efficiency, it is regarded as one of the superior isolation techniques for tocopherols concentration and drug development (Mahmoud et al., 2021; Pouran et al, 2021).

In this study, adsorption performance models are employed in investigating the dynamic behaviour of tocopherol adsorption utilizing silica gel as the adsorbent. The adsorption is based on equilibrium correlations governing the adsorption system, the adsorption mechanism and kinetics, and the conservation thermodynamics associated with the adsorption process. The adsorption models are evaluated and statistically validated to fit the adsorption data to further elucidate the adsorption of tocopherols present in PFAD on silica gel.

This work aims at using PFAD as a raw material for the production of tocopherols, with the production itself evolving from the extraction and enrichment of tocopherols present in PFAD using the adsorption technique as a flexible option. This study also tends to demonstrate a value-added approach for PFAD utilization, especially for the palm oil industry (Serbinova et al., 1991), the pharmaceutical industry and natural products research as a whole. Furthermore, in terms

of effective engineering designs and operation of adsorption systems, this study will be useful for the quantitative description and comparisons of the adsorption equilibrium models.

2.0 Material and methods

2.1 Materials

Reference standards of tocopherol were purchased from Sigma Aldrich Chemical Company (St. Louis, MO, USA). All other reagents were of analytical grade. The palm fatty acid distillate (PFAD) was obtained from Presco Palm Oil Processing Industry located at Obaretin, Edo State in Nigeria in its unadulterated form. The PFAD sample was stored in the refrigerator at a temperature of ≤ 4 ℃ till further analysis. The adsorbent used in this study was silica gel and the solvents used were of High-performance liquid chromatography (HPLC) grade. These were purchased at Onitsha Market in Anambra State, Nigeria. Experiments were performed in the Multi-Purpose Laboratory, Ahmadu Bello University, Zaria.

2.2 Adsorbent Enhancement

The adsorptive capacity of silica gel (adsorbent) was modified according to the method explained in the work of Huang et al., (2017). A solution referred to as a composite modifier was prepared with ethyl alcohol, *n*-heptane and trimethylchlorosilane (volume ratio of 1:13:1). A substantial amount of silica gel was dried in a vacuum drier which was heated at 80 ℃ for 5hr and then immersed into the modifier for 1hr at room temperature. Afterwards, the mixture containing the modifier and the silica gel was put in a microwave oven under the following exposure conditions according to equipment design: microwave power 700W, oven temperature 60 ℃ and exposure time of 30min. The mixture was left to cool at room temperature for another 9hrs. Filtration of the modified silica gel sample followed after cooling, and the sample was washed with distilled water several times until neutrality was obtained. The resultant sample was dried at 80 ℃ until its weight was invariable.

2.2.1 Characterization of Adsorbent

The silica gel samples were characterized to reveal information through the use of the Scanning Electron Microscopy (SEM) instrument for microanalysis, and the Fourier Transform Infrared (FTIR) instrument for the identification of organic polymeric materials present in the samples. SEM images were recorded on a Philips XL electron microscope operated at 15 kV. FTIR spectra of silica gel were recorded with a Fourier transform infrared spectroscopy instrument (Model Thermo Nicolet Nexus) in the range of 4000 – 400 $cm^{-1}$and at 4 cm^{-1} the resolution was applied to measure the IR absorbance of the KBr disk containing the samples. The specific surface area, pore volume and pore sizes of the silica gel was measured by the adsorption method in the presence of nitrogen gas, using the Autosorb-IQ2-MP-XR-VP analyser instrument 77 K (Rahman et al., 2015; Khadangi and Azzi, 2019). The silica gel sample was dried at 90 ℃ for 2 hrs, and the adsorption isotherms are obtained at -196.15 ℃. Furthermore, the specific surface area was calculated from the Brunauer–Emmett–Teller (BET) method at $P/P_0 < 0.3$. Pore volume and pore size distribution, total pore volume (V_t) were estimated from the adsorbed amount at a relative pressure (p/p_0) of 0.95. Furthermore, the micropore volume (V_m) and micro-pore surface area (S_m) were also determined, and the average pore diameter (P_D) were evaluated from the tabular data section of the measuring instrument software.

2.3 Determination of Tocopherol in PFAD

PFAD was melted at 38℃. The melted sample was centrifuged at $1400 \times g$ to separate water from the PFAD. About 15 g of PFAD sample was extracted from the centrifuge tube and thereafter dissolved in 30 ml ethanol. The sample was then neutralized with 0.5 N NaOH to the phenolphthalein end-point. Distilled water (50 ml) and 100 ml n-hexane were added and the sample was agitated for 1 min. The mixture was then transferred into a separatory funnel and allowed to stand as two distinct layers formed. The bottom layer primarily made up of FFA salts was extracted for analysis while the top layer containing tocopherols was retained. Furthermore, the top layer was centrifuged at $2500 \times g$ for 1min to separate the water. The hexane layer was transferred into a 250 ml round-bottom flask and heated at 60 ℃ under vacuum.

2.4 Analysis of Tocopherol Content

The sample containing tocopherol was determined using HPLC equipment. A known amount (0.05 g) of the sample (PFAD) was dissolved in 2 ml of n-hexane and 5µl of the mixture was injected into HPLC equipment (Agilent Technologies). The HPLC (Agilent 1100 series) set at reverse phase mode also operated at Agilent isocratic conditions

with a stack configuration of the solvent cabinet, vacuum degasser, HP-1100 pump system, and an auto-sampler, column compartment and fluorescence detector (G1321 A FLD). The column was a Hypersil ODS, 125 mm × 4 mm internal diameter with 5μm particles; a capillary length of 150 mm and 0.17 mm i.d. The mobile phase was a mixture of methanol and water (95:5, v/v) and eluted at a flow rate of 1.0 ml/min. The analytical column was set at 290 nm excitation wavelength and 325 nm emission wavelength. The total separation time was 10mins. The tocopherols were identified by comparison of retention times of the standards of α, γ and δ- tocopherols. The Peak area was used for quantification. In this work, the sum of concentrations of α, γ and δ- tocopherols was used as the total tocopherol content in the PFAD.

2.5 Tocopherols Quantification

External calibration was performed before analyses of edible plant oil by injecting different concentrations into the column. Standard curves (peak area vs concentration) were calculated by linear regression analysis. Injections in triplicate were made at each concentration for both standards and samples. The calibration curves were constructed using standard solutions of α, γ- and δ- tocopherols and used for quantification. The total tocopherol content is expressed in percentage as total tocopherol content.

2.6 Preconcentration of PFAD

PFAD was modified following the preconcentration steps explained by Chu et al., (2002). A mass of 25g of PFAD was dissolved in 50 ml of ethanol and was neutralized using 0.5N sodium hydroxide to attain a phenolphthalein end-point. 50 ml of distilled water and 150 ml of n-hexane were then added and the sample was agitated for 1 min. the sample matrix was then allowed to stand for phase separation in a separating funnel. The n-hexane layer was extracted. The sample was re-extracted with an additional 100 ml of n-hexane at least four times more. In respective instances, the accumulated mixture was washed four times with 150 ml of distilled water to remove sodium hydroxide and soap compounds. The extract was then centrifuged at 3000×g for 1 min and residual water was drained before transferring the pure extract to a 500 ml round-bottom rotary evaporator flask. The heating condition of the evaporator was at 50℃ under vacuum.

2.7 Equilibrium Adsorption Experiment

The batch equilibrium adsorption experiment followed a similar approach described by Chu et al., (2002) sample of neutralized PFAD (3 g) was dissolved in n-hexane to give a stock solution with the following concentrations of tocopherol: 6.2E-02, 12.2E-02, 19.0E-02 and 26.5E-02 (mg/ml). The batch mode adsorption studies also entail equilibrating an accurately weighed amount of adsorbent (silica gel) in proportions of 0.5, 1.0, 2.0 and 2.5 g, with 50 ml of sample solutions of known initial tocopherol concentration in 100 ml sealed conical flasks. The samples were flushed with nitrogen gas to avoid the oxidation of tocopherol during the adsorption experiment. Then, samples were agitated using magnetic stirrer equipment at 180 revolutions per minute (rpm) and 50 ℃ for 30min. After attaining equilibrium, the contents of the flask were filtered using Whatman 0.45μm nylon membrane filters and subsequently analyzed for residual concentration of tocopherol in the solution. The concentration of the adsorbed tocopherol was calculated as the difference between the known total amount of tocopherol adsorbed and the amount measured in the solution after equilibrium was attained. The effect of temperature was studied at different temperature settings (35, 40, 45, and 50 ℃). For the effect of agitation rate, values ranged from 120 rpm to 180 rpm. Tocopherol concentration was determined using HPLC equipment as described by Chu et al., (2002).

2.8 Adsorption Model Fitting and Analysis

Nonlinear adsorption models and analyses were used to fit the experimental data obtained from adsorption equilibrium. Statistical analyses were done using Microsoft Excel 2016 Solver Add-in. A goodness-of-fit approach was tested across seven (7) error functions to obtain the best model that fits the experimental data (**Table 1**).

Table 1: List of Error Functions for Goodness-of-Fit Evaluation

Error Function	Equation	Equation Number	Reference
Squared errors/Sum Square of Errors (ERRSQ/SSE)	$\sum_{i=1}^{n}\left(q_{e,exp.}-q_{e,pred}\right)_i^2$	(1)	(Namasivayam and Ranganthan, 1995; Foo and Hameed, 2010)
Coefficient of determination R^2	$\frac{q_{e,exp}-\overline{q_{e,pred}}^2}{\sum\left(q_{e,exp}-\overline{q_{e,pred}}^2\right)+\left(q_{e,exp.}-q_{e,pred}\right)^2}$	(2)	(Nebaghe et al., 2016; Draper and Smith, 2016)
Spearman's Correlation Coefficient (r_s)	$1-\frac{6\sum_{i-1}^{n}\left(q_{e,exp.}-q_{e,pred}\right)_i^2}{n(n-1)^2}$	(3)	(Lehman, 2005; Ayawei et al., 2017)
Sum of Absolute Error (EABS)	$\sum_{i=1}^{n}\left\lvert q_{e,exp.}-q_{e,pred}\right\rvert$	(4)	(Nebeghe et al., 2016; El Nemr et al., 2010)
Hybrid Fractional Error (HYBRID)	$\frac{100}{n-p}\sum_{i=1}^{n}\left[\frac{q_{e,exp.}-q_{e,pred}}{q_{e,exp}}\right]$	(5)	(Ayawei et al., 2017)
Marquardt's Percent Standard Deviation (MPSD)	$100\sqrt{\frac{1}{n-p}\sum_{i=1}^{n}\left(\frac{q_{e,exp.}-q_{e,pred}}{q_{e,exp}}\right)_i^2}$	(6)	(Saadi et al., 2015)
Nonlinear Chi-Square χ^2	$\sum_{i=1}^{n}\frac{\left(q_{e,exp.}-q_{e,pred}\right)^2}{q_{e,exp}}$	(7)	(El Nemr et al., 2010)

3.0 Results and Discussions

3.1 Adsorbent Modification and Characterization

Silica gel was modified to enhance its adaptability, and also improve its hydrophobic and other inherent adsorptive properties. The enhanced hydrophobicity was a result of a chemical reaction that occurred between the silica particles and the composite modifier (ethyl alcohol, n-heptane and trimethylchlorosilane, in a volumetric ratio of 1:13:1).

3.1.1 Morphological Analysis of Adsorbent

Scanning electron microscope (SEM) images of ordinary and modified silica gel are shown in **Figures 1a** and **1b** respectively. By comparing topography, the image of the ordinary silica gel (**Figure 1a**) depicted a relatively smooth surface. Some structural clusters can be seen on the surface of the modified silica gel (**Figure 1b**).

The result of the modification of silica revealed a rough, tightly packed surface arrangement present in form of intervening granules when compared with the precursor (**Figure 1b**). Having tightly packed morphology indicated that the modified structure was fit for adsorption. Furthermore, from **Figure 1b**, it can be inferred that the average pore size of the modified sample decreased slightly, as a result of the modification technique applied.



Figure 1a: SEM imagery of ordinary silica gel

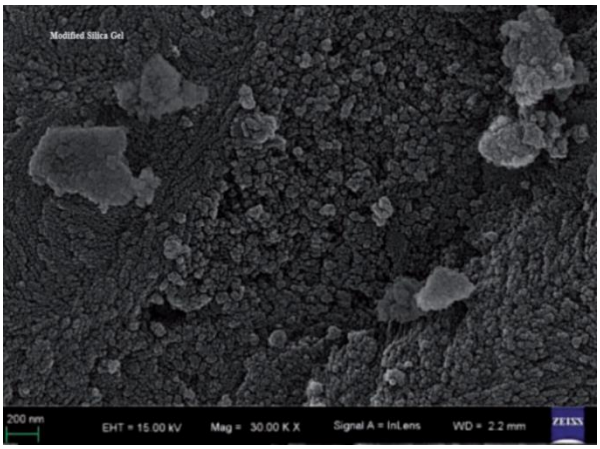


Figure 1b: SEM imagery of modified silica gel

3.1.2 Surface Structure of Adsorbent

The values of the respective samples' BET areas and average pore sizes are listed in **Table 2**. As shown in the list, the value of BET surface area (S_{BET}) and the average pore size of ordinary silica gel was higher compared to that of the modified silica gel. It can be seen in **Table 2** that the values of S_{BET} and pore diameter P_D reduced from 464 to 433 m^2/g, and from 7.08 to 5.49 nm, respectively, because of the extent of modification in the internal structure of silica. More so, other surface structure parameters such as the micro-pore volumes (V_m) and total pore volume (V_t) respectively have reduced values when both adsorbents are compared. However, in **Table 2** the micro-pore surface areas (S_m) increased after the modification process.

Table 2: Surface structure parameters of silica gel adsorbent

Sample	$S_{BET}\ (m^2/g)$	$S_m\ (m^2/g)$	$V_t\ (c\,m^3/g)$	$V_m\ (cm^3/g)$	$P_D\ (nm)$
Silica Gel	464	900	0.81	0.79	7.08
Modified Silica Gel	433	1023	0.64	0.75	5.49

3.1.3 FT-IR Analysis of Adsorbent

The infrared patterns of the silica gel and modified silica gel samples are shown in **Figure 2.** The signals located at 3500.76 cm^{-1} and 1650.09 cm^1 are assigned to anti-symmetry vibrations of Si-OH (Horvath et al., 2005). The corresponding intensity weakened significantly for the modified silica sample compared with the original sample, indicating the removal of the –OH group by the treatment. After the modification, the manifestation of new signs at 1095.44 and 470.97 cm^1 caused by Si-O-Si anti-symmetric stretching vibration can be seen. Moreover, Si-O stretching vibration at 802.34 cm^1 and C-C vibration peak at 969.23 cm^1 also appeared, showing the enhancement of hydrophobicity of the modified silica sample.

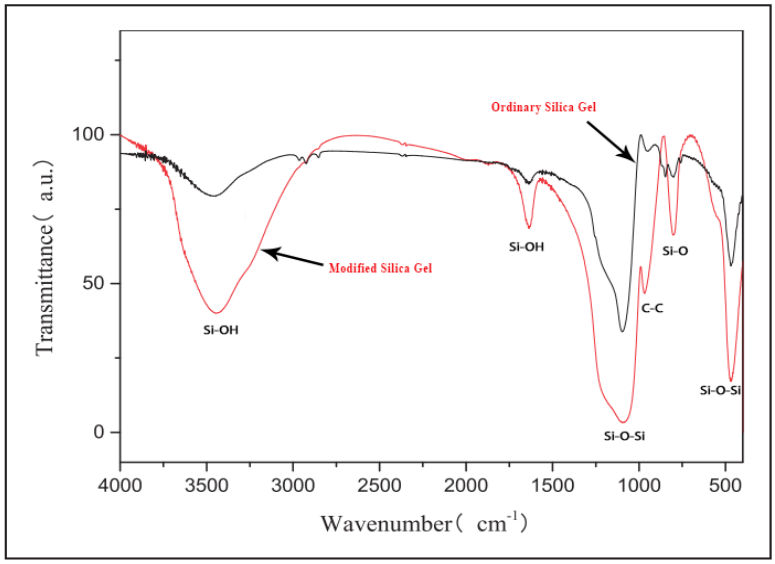


Figure 2: FT-IR patterns for ordinary and modified silica gels

3.2 Equilibrium Adsorption Isotherms

To establish appropriate correlations between the equilibrium curves of each sample, four isotherms namely the Langmuir, Freundlich, Redlich-Peterson and Koble-Corrigan were applied to determine which model best described the adsorption process.

The Langmuir isotherm possesses dual equilibrium constants, K_L(ml/mg) and a_L (ml/mg). According to Chu et al., (2004), the Langmuir model for dilute solution may be represented by **Eq. (8)**:

$$q_e = \frac{K_L C_e}{1 + a_L C_e} \tag{8}$$

where q_e is the amount of adsorbate in the adsorbent at equilibrium (mg/g), and C_e is the equilibrium concentration (mg/ml) of the adsorbate.

The values of these parameters were determined from the fitting of nonlinear regression analysis and the results obtained were summarized in **Table 3** for the Langmuir Isotherm**.** It was observed that changes in the Langmuir constants exhibited an irregular pattern around the reaction parameters. Nevertheless, the value of Q_0 decreased as the temperature of the system increased, and decreased as agitation speed decreased. An increase in temperature aided the adsorption process thereby increasing the adsorption capacity of the adsorbent. High agitation speed allowed for relatively easy uptake of tocopherol onto the adsorbent. On the other hand, the value of the Langmuir equilibrium constants increased as the mass of the adsorbent reduced. This is attributed to the availability of extra pore space on the surface of the adsorbent.

Table 3: Summary of nonlinear regression analysis for the Langmuir isotherm

Adsorption System Parameter	Langmuir Isotherm Parameters K_L (ml/mg)	a_L (ml/mg)	$Q_0 = {K_L}/{a_L}$ (mg/g)	R^2	ERRSQ/SSE
Temperature ℃					
50	30.3726	1326.3144	0.0229	0.9996	1.7061E-07
45	17.0659	484.9834	0.0352	0.9986	1.4832E-06
40	13.9171	282.0861	0.0493	0.9952	9.9273E-06
35	31.0537	516.0744	0.0602	0.9315	2.54E-04
Agitation Speed (rpm)					
180	8.5322	149.9109	0.0569	0.9946	1.52E-05
160	5.6197	140.4056	0.0400	0.9996	5.16E-07
140	7.0273	232.7140	0.0302	0.9991	7.06E-07
120	4.0269	201.6196	0.0200	0.9961	1.33E-06
Mass of Adsorbent (g)					
1.00	4.9952	99.8685	0.0500	0.9955	8.69E-06
0.75	6.4547	120.6721	0.0535	0.9955	1.36E-05
0.50	13,9355	271.1792	0.0514	0.9944	1.53E-05
0.25	19.1736	346.4842	0.0553	0.9869	4.7E-05

Theoretical maximum monolayer capacity, Q_0 (mg/g) = ${K_L}/{a_L}$

The Freundlich isotherm is an empirical model that deals with the adsorption of a species on a heterogeneous surface. The Freundlich model parameters were computed from **Eq. (9)**, which is the nonlinear model type (Chu et al., 2004).

$$q_e = K_F C_e^{n_F} \quad (9)$$

where $n_F = 1/n$, and n_F is a function of adsorption intensity n; it also indicates the relative distribution of energy and heterogeneity of the adsorbent sites. K_F is the adsorption capacity (L/mg) and *1/n* is the adsorption intensity; this also indicates the relative distribution of the energy and the heterogeneity of the adsorbate sites.

Similar to the Langmuir isotherm, the Freundlich isotherm has two constants indicated as K_F and n_F, constants for a given adsorbate and adsorbent respectively at the particular temperature used to define the adsorption mechanism, and data are shown in **Table 3.**

In **Table 4**, as n_F increased, *n* decreased which is true about inverse relationships. If the Freundlich exponent term n_F is less than 1, it will indicate that as sorbate concentrations increased around the adsorbent, sorption of additional molecules on the adsorbent surface will become more difficult (Proctor and Toro-Vazquez, 2009). However, this is not the case in this study as the values n_F were mostly greater than unity (except when the adsorbent mass was 0.25g and 0.5g), hence the sorption of additional solute molecules found their way easily onto the adsorbent surface. It was observed that the values n_F increased as the adsorption temperature increased. This indicated that at high adsorption temperature sorbate concentration reduced in areas around the adsorbent and this favoured the adsorption process because sorbate molecules efficiently pinged on the surface of the adsorbent (Van der Bruggen, 2014). In terms of agitation speed, n_F values decreased as agitation speed increased. Furthermore, as seen in **Table 4**, a low agitation rate has resulted in a high adsorption efficiency. Also, the experimental result revealed that as the mass of the adsorbent decreased, n_F values decreased. This indicated that adsorption proceeded as there were more pore spaces on the adsorbent as more concentrations of the adsorbate (tocopherol) were around the binding site of the adsorbate.

The K_F the term implies that the energy of adsorption on the surface of the adsorbent is independent of surface coverage even though there are many binding sites on the surface of the adsorbent (Proctor and Toro-Vazquez, 2009; Van der Bruggen, 2014). K_F values decreased as the adsorption temperature increased. This indicated that the adsorption capacity of the adsorbent was hindered at high temperatures. K_F values decreased as the mass of the adsorbent decreased. This indicated a reduction in the number of binding sites as the surface of the adsorbent was rapidly occupied by sorbate molecules as the reaction proceeded (Proctor and Toro-Vazquez, 2009). In another case, K_F values increased as agitation speed increased (**Table 4**). This indicated that the energy of adsorption on the surface of the adsorbent was balanced by the rate of agitation provided for the adsorption of tocopherol onto the surface of the adsorbent.

Table 4: Summary of nonlinear regression analysis for the Freundlich isotherm

Adsorption System Parameter	Freundlich Isotherm Parameters			R^2	ERRSQ/SSE
	K_F $(mg/g)(ml/g)^n$	n_F	n		
Temperature ℃					
50	0.0277	14.5171	0.0689	0.9865	6.07E-05
45	0.0471	8.7449	0.1143	0.9735	2.78E-05
40	0.0778	5.6261	0.1777	0.9910	1.85E-05
35	0.0997	5.5620	0.1798	0.9995	1.91E-06
Agitation Speed (rpm)					
180	0.1052	3.9259	0.2547	0.9550	1.24E-04
160	0.0691	4.2287	0.2365	0.9646	4.72E-05
140	0.0485	5.3885	0.1856	0.9811	1.39E-05
120	0.0320	5.1107	0.1957	0.9601	1.34E-05
Mass of Adsorbent (g)					
1.00	0.1294	2.7200	0.3676	0.9507	9.42E-05
0.75	0.1149	3.2367	0.3090	0.9716	7.33E-05
0.50	0.1003	0.2449	4.0833	0.9655	9.30E-05
0.25	0.0898	0.1920	5.2083	0.9835	4.94E-05

Table 5: Summary of nonlinear regression analysis for the Redlich-Peterson isotherm

Adsorption System Parameter	Redlich-Peterson Isotherm Parameters			R^2	ERRSQ/SSE
	K_R (ml/mg)	a_R (ml/mg)	n_R		
Temperature ℃					
50	28.3270	1265.3340	1.0069	0.9997	1.28E-07
45	15.3823	458.2034	1.0173	0.9989	1.11E-06
40	22.1973	365.3875	0.9211	0.9995	1.09E-06
35	20.0000	188.0000	0.8219	0.9432	4.08E-04
Agitation Speed (rpm)					
180	7.2124	157.1933	1.0754	0.9964	1.00E-05
160	5.1610	134.4638	1.0296	0.9999	9.87E-08
140	6.7286	223.5617	1.0044	0.9992	5.90E-07
120	3.1815	194.2330	1.0773	0.9988	4.03E-07
Mass of Adsorbent (g)					
1.00	3.9377	128.4465	1.1753	0.9987	2.05E-06
0.75	7.9166	127.5985	0.9400	0.9959	1.07E-05
0.50	17.9354	289.3496	0.9429	0.9974	6.93E-06
0.25	41.1270	572.9607	0.8952	0.9971	8.61E-06

The Redlich-Peterson isotherm was also employed to study the dependence of the quantity of tocopherol adsorbed at equilibrium on the concentration of tocopherol in the bulk phase. The nonlinear equations of the model are represented by **Eq. (10)** (Ayawei et al., 2017):

$$q_e = \frac{K_R C_e}{1 + a_R C_e^{n_R}} \quad (\mathbf{10})$$

Plotting $ln\left({C_e}/{q_e}\right)$ versus $ln\ C_e$ allows the distribution of Redlich-Peterson constants, n_R and a_R from the slope and intercept, respectively.

Furthermore, the Koble-Corrigan Isotherm (Koble and Corrigan, 1952) was adopted to study the equilibrium adsorption relationship from experimental data. The nonlinear form of the model is represented by **Eq. (11)**.

$$q_e = \frac{AC_e^{n_{KC}}}{1 + BC_e^{n_{KC}}} \quad (\mathbf{11})$$

The Koble-Corrigan isotherm model constants, A, B, and n_{KC} are evaluated from linear plots using a trial-and-error optimization technique (Ayawei et al., 2017).

Table 5 and **Table 6** respectively show the summaries of nonlinear regression analyses for the Redlich-Peterson and Koble-Corrigan isotherm. Nevertheless, both models are composed of three parameters – double isotherm constants, and an isotherm exponent term (n_R and n_{KC} respectively). These isotherms have the combined features of the Langmuir and Freundlich isotherm models.

The applicability of these three-parameter isotherm models to the adsorbate–adsorbent system was used to validate the effect of both monolayer adsorption and heterogenous surface conditions that were presumably existent under the experimental conditions applied. The deterministic factor of whether either model is Langmuir-favoured or Freundlich-favoured is the value of the isotherm's exponent values. Both three-parameter isotherms, in terms of the isotherm model exponent values, were evaluated (Chu et al., 2004). As inferred by **Table 5**, the Redlich-Peterson isotherm model was transiting into the Langmuir form while the Koble-Corrigan isotherm model exponent term values were within their range of values. This trend indicated that the three-parameter models possess the ability to explain both monolayer adsorption and heterogenous surface conditions of the adsorbent. These were the core system fundamentals described by the models themselves. The adsorption of tocopherol on the modified silica gel was thus a complex process, having more than one mechanism. Apart from the models' exponent values, respective model constants varied accordingly relative to the system parameters (adsorption temperature, agitation speed and mass of adsorbent).

Table 6: Summary of nonlinear regression analysis for the Koble-Corrigan isotherm

Adsorption System Parameter	Koble-Corrigan Isotherm Parameters			R^2	ERRSQ/SSE
	A	n_{KC}	B		
Temperature ℃					
50	0.4297	0.3342	15.1123	0.9925	3.39E-06
45	0.8671	0.4972	21.2950	0.9894	1.13E-05
40	1.7989	0.6385	32.2515	0.9998	3.35E-07
35	0.6786	0.4317	8.0160	0.9904	3.98E-05
Agitation Speed (rpm)					
180	1.4513	0.6817	21.5082	0.9828	4.84E-05
160	1.0363	0.6853	22.0795	0.9919	1.09E-05
140	0.5335	0.5347	14.1176	0.9928	5.25E-06
120	0.3404	0.5460	13.7310	0.9805	6.55E-06
Mass of Adsorbent (g)					
1.00	6.3086	1.0488	126.9965	0.9961	7.67E-06
0.75	1.5722	0.7392	25.2214	0.9962	1.03E-05
0.50	1.2941	0.6152	20.5414	0.9934	1.82E-05
0.25	1.2975	0.5547	20.0023	0.9986	4.51E-06

3.3 Adsorption Isotherm Model Fitting

A summary of the error function test on adsorption isotherms is given in **Table 7**. Using the error functions, the findings demonstrated in **Table 7** helped to estimate the errors associated with each model, and this statistically clarified which model best fit the experimental data. It can be inferred from **Table 7** that the values of ERRSQ/SSE, EABS, and HYBRID for the Koble-Corrigan isotherm model are less than the values of the same error function for other models. However, the EABS or HYBRID value of a negative number is also its absolute value (Nebeghe et al., 2016; El Nemr et al., 2010; Ayawei et al., 2017). Hence their absolute values were considered during error function evaluations. Based on the proportion of total variation of outcomes explained by any of the isotherm models, i.e., $\boldsymbol{R^2}$ (Nebaghe et al., 2016; Draper and Smith, 2016)**,** **Table 7** also shows that the value of the $\boldsymbol{R^2}$ for Koble-Corrigan is higher when compared to the values of $\boldsymbol{R^2}$ associated with the other isotherms. This suggests that the Koble-Corrigan isotherm had the highest predictive power on the experimental data than that of the other isotherms. The Langmuir isotherm possessed the lowest MSPD value, which defined the extent of deviation of the predicted q_e values for each isotherm (Ayawei et al., 2017; Seidel and Gelbin, 1988; Al-Ghouti and Da'ana, 2020). $\boldsymbol{\chi^2}$ measures the sum of the square difference between the experimental and the calculated data, with each squared difference divided by its corresponding value (calculated from the models). A small χ^2 the value indicates its similarities while a large number represents the variation of the experimental data (Boulinguiez et al., 2008). As shown in **Table 7**, the computation of the $\boldsymbol{\chi^2}$ error function reveals that the Koble-Corrigan isotherm had the smallest deviation from experimental data. Lastly, $\boldsymbol{r_s}$ values for all isotherms units (**Table 7)**. Therefore, the $\boldsymbol{r_s}$ error function yielded no meaningful comparison that decided the best-fit model.

Table 7: Summary of error functions test on isotherms

Isotherm	Error Function						
	ERRSQ/SSE	$\boldsymbol{R^2}$	$\boldsymbol{r_s}$	**EABS**	**HYBRID**	**MPSD**	$\boldsymbol{\chi^2}$
Langmuir	3.6351E-05	0.9910	1	0.0012	0.7932	15.4059	0.0009
Freundlich	5.5344E-05	0.9859	1	-0.0006	-0.9938	6.8287	0.0012
Redlich-Peterson	2.2100E-06	0.9994	1	4.8200E-05	0.0472	1.0686	4.0000E-05
Koble-Corrigan	8.5100E-07	0.9999	1	9.2600E-05	-0.0159	0.5976	1.4500E-05

The goodness-of-fit test was adopted to compare the experimental data with the data expected under the models using the error functions as some fit discrepancy measures, and this is graphically represented in **Figure 3.3**. As shown in **Figure 3.3**, the plots involved model comparison of the experimental data with the empirical adsorption isotherm as a function of q_e and C_e. The result is depicted in **Figure. 3.3** shows the Koble-Corrigan isotherm model was the best-fit model for predicting experimental data.

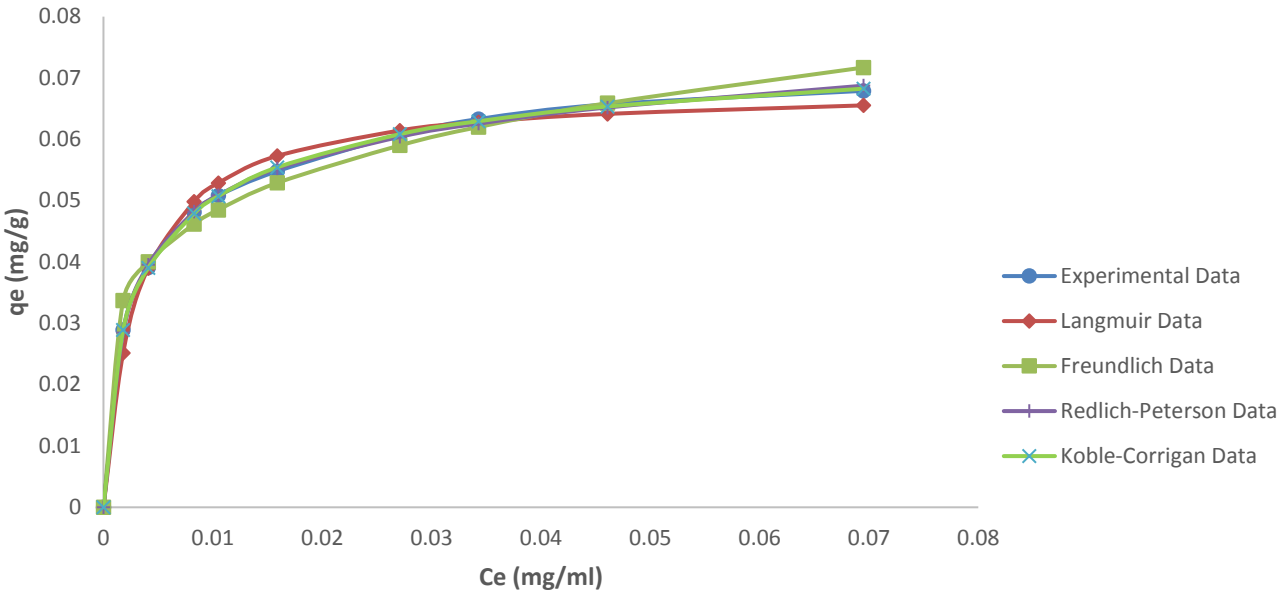


Figure 3: Goodness-of-fit chart

4.0. Conclusion

A simple novel approach to selectively extract tocopherols from PFAD was studied. In prior batch adsorption studies, the process consisted of several steps, such as enhancement of the adsorptive capacity of the adsorbent (silica gel), the determination and the analysis of tocopherol content in PFAD, quantification of tocopherol, pre-concentration of the PFAD, the adsorption of tocopherol onto modified silica gel, and adsorption isotherm model fitting and analysis. In the adsorbent modification step, a composite modifier (ethyl alcohol, n-heptane and trimethylchlorosilane) used in treating the silica gel enhanced its hydrophobicity. Several analyses such as SEM, FT-IR and BET surface area were performed to reveal the degree of adsorbent modification. In the batch adsorption process, four isotherms namely the Langmuir, the Freundlich, the Redlich-Peterson and the Koble-Corrigan were applied in the modelling of experimental adsorption isotherm data. Seven statistical metrics which served as error functions to evaluate the goodness-of-fit were the validation criteria for choosing the best-fit isotherm model. The Koble-Corrigan isotherm model possessed the lowest pure-effect of aggregated error functions, thus manifested as the best-fit model with better prediction power in describing the equilibrium adsorption tocopherol in a batch process using modified silica gel. This research is hoping to contribute to the direction of adsorption system modelling for the extraction of bioactive substances from by-products of vegetable oil refining. This novel, cheap and simple extraction technique permits the selectivity and efficient adsorption of tocopherols from PFAD.

References

Aggarwal B. B., Sundaram C., Prasad S., Kannappan R. 2010. Tocotrienols, the vitamin E of the 21st century: its potential against cancer and other chronic diseases, Biochem. pharmacol. 2010, 80: 1613–1631.

Al-Ghouti, M. A., and Da'ana, D. A. 2020. Guidelines for the use and interpretation of adsorption isotherm models: A review. Journal of Hazardous Materials 2020. Elsevier B.V. https://doi.org/10.1016/j.jhazmat.2020.122383

Ayawei, N., Ebelegi, A. N., and Wankasi, D. 2017. Modelling and Interpretation of Adsorption Isotherms. Journal of Chemistry 2017. https://doi.org/10.1155/2017/3039817

Boulinguiez B., Le Cloirec P., and Wolbert D. 2008. Revisiting the determination of Langmuir parameters application to tetrahydrothiophene adsorption onto activated carbon, Langmuir, 24: 6420–6424.

Chu B.S, Baharin B.S., Che Man Y.B., and Quek S.Y. 2004. Separation of vitamin E form palm fatty distillate using silica: I Equilibrium of batch adsorption. Journal of food engineering, 62: 97 – 103.

Chu B.S., Baharin B.S. and Quek S.Y. 2002. Factors Affecting Pre-concentration of Tocopherols and Tocotrienols from Palm Fatty Acid Distillate by Lipase-Catalyzed Hydrolysis. Food Chemistry, 79: 55-59.

Draper N. R., Smith H. 1998. Applied Regression Analysis. Wiley-Interscience 1998, ISBN 978-0-471-17082-2.

Eitenmiler R, Lee J. 2014. Vitamin E: Food Chemistry, Composition, and Analysis, Marcel Dekker Inc., New York, pp. 1-13.

El Nemr, A., El-Sikaily, A., Khaled, A. 2010. Modeling of adsorption isotherms of Methylene Blue onto rice husk activated carbon. Egypt. J. Aquat. Res., 36 (3): 403–425.

El Nemr, A., El-Sikaily, A., Khaled, A. 2010. Modeling of adsorption isotherms of Methylene Blue onto rice husk activated carbon. Egypt. J. Aquat. Res., 36 (3): 403–425.

Foo K.Y. and Hameed B.H. 2010. Insights into the modelling of adsorption isotherm systems. Chemical Engineering Journal, 156: 2-10.

Horvath E, Kristo f. J., Nasser H. 2005. Investigation of SnO_2 thin film evolution by thermos-analytical and spectroscopic methods. Applied Surface Science, 242: 13–20.

Huang W., Jixing X., Bo T., Hongning W., Xiaobin T. and Aihua L. 2017. Adsorption performance of hydrophobically modified silica gel for the vapors of n-hexane and water. Adsorption Science and Technology, 36 (3-4): 888-903.

Khadangi, F., & Azzi, A. 2019. Vitamin E – The Next 100 Years. IUBMB Life. Blackwell Publishing Ltd. https://doi.org/10.1002/iub.1990

Koble R. A., Corrigan T. E. 1952. Adsorption isotherms for pure hydrocarbons, Ind. Eng. Chem., 44: 383–387.

Lee, G. Y., & Han, S. N. 2018. The role of vitamin E in immunity. Nutrients, MDPI AG. https://doi.org/10.3390/nu10111614

Lehman Ann. 2005. Jmp for Basic Univariate and Multivariate Statistics: A Step-by-step Guide. Cary, NC: SAS Press, 123. ISBN 978-1-59047-576-8.

Lewis, E. D., Meydani, S. N., & Wu, D. 2019. Regulatory role of vitamin E in the immune system and inflammation. IUBMB Life, 71(4): 487–494. https://doi.org/10.1002/iub.1976

Lewis, E. D., Meydani, S. N., & Wu, D. 2019. Regulatory role of vitamin E in the immune system and inflammation. IUBMB Life, 71(4): 487–494. https://doi.org/10.1002/iub.1976

Liu D., Shi J., Posada L. R., Kakuda Y., & Xue S. J. 2008. Separating Tocotrienols from Palm Oil by Molecular Distillation. Food Reviews International 2008, 24(4): 376–391. doi:10.1080/87559120802303840

Mahmoud, D.K., Salleh, M.A, and Karim, W.A. 2021. Langmuir Model Application on Solid-Liquid Adsorption Using Agricultural Wastes: Environmental Application Review, Journal of Purity, Utility Reaction and Environment, 1: 170-199

Namasivayam, C. and Ranganathan K. 1995. Removal of Cd (II) from wastewater by adsorption on “waste” Fe(III)/Cr(II) hydroxide. Water Research, 29: 1737 – 1744.
Nebaghe, K., El Boundati, Y., Ziat, K., Naji, A., Rghioui, L., Saidi, M. 2016. Comparison of linear and non-linear method for determination of optimum equilibrium isotherm for adsorption of copper (II) onto treated Martil sand. Fluid Phase Equilib., 430: 188–194.

Ng W.-K., Lim P.-K., & Boey P.-L. 2003. Dietary lipid and palm oil source affects growth, fatty acid composition and muscle α-tocopherol concentration of African catfish, Clariasgariepinus. Aquaculture, 215(1-4): 229–243. doi:10.1016/s0044-8486(02)00067-4

Ngoc Doan, P., Tan, T., Siow, L. F., Tey, B. T., Chan, E. S., Tang, T., Lee, Y. 2021. Dry Fractionation Approach in Concentrating Tocopherols and Tocotrienols from Palm Fatty Acid Distillate: A Green Pretreatment Process for Vitamin E Extraction. Journal of the American Oil Chemists' Society, 98(6): 609–620. doi:10.1002/aocs.12488

Pouran Pourhakkak, Ali Taghizadeh, Mohsen Taghizadeh, MehrorangGhaedi, SepahdarHaghdoust. 2021. Chapter 1 - Fundamentals of adsorption technology, Editor(s): MehrorangGhaedi, Interface Science and Technology, Elsevier, 33: 1-70, ISSN 1573-4285, ISBN 9780128188057, https://doi.org/10.1016/B978-0-12-818805-7.00001-1.

Proctor, A., & Toro-Vazquez, J. F. 2009. The Freundlich Isotherm in Studying Adsorption in Oil Processing. In Bleaching and Purifying Fats and Oils: Theory and Practice, pp. 209–219. Elsevier Inc. https://doi.org/10.1016/B978-1-893997-91-2.50016-X

Rahman N.A., Widhiana I., Juliastuti S.R., Setyawan H. 2015. Synthesis of mesoporous silica with controlled pore structure from bagasse ash as a silica source. Colloids and Surface A: Physicochem. Eng. Aspects, 476: 1 -7.

Rakmi, A.R. and T. Herawan 2000. Properties of biosurfactant enzymatically prepared from fructose and palm fatty acid. J. Oil Palm Res., 12(1): 117-122.

Rizvi, S., Raza, S. T., Ahmed, F., Ahmad, A., Abbas, S., & Mahdi, F. 2014. The role of Vitamin E in human health and some diseases. Sultan Qaboos University Medical Journal.

Saadi, R., Saadi, Z., Fazaeli, R., Fard, N. 2015. Monolayer and multilayer adsorption isotherm models for sorption from aqueous media. Korean J. Chem. Eng., 32 (5): 787–799.

Seidel A. and Gelbin D. 1988. On applying the ideal adsorbed solution theory to multicomponent adsorption equilibria of dissolved organic components on activated carbon, Chem. Eng. Sci., 43: 79–89.

Serbinova, E., Kagan, V., Han, D., & Packer, L. 1991. Free radical recycling and intramembrane mobility in the antioxidant properties of alpha-tocopherol and alpha-tocotrienol. Free Radical Biology and Medicine, 10(5): 263–275. https://doi.org/10.1016/0891-5849(91)90033-Y

Sharma, S.K.; Bansal, S.; Mangal, M.; Dixit, A.K.; Gupta, R.K.; Mangal, A.K. 2015. Utilization of food processing by-products as dietary, functional, and novel fiber: A review. Crit. Rev. Food Sci. Nutr., 56, 1647–1661.

Upadhyay J. and Misra K.. 2009. Towards the interaction mechanism of tocopherols and tocotrienols (vitamin E) with selected metabolizing enzymes. Bioinformation 2009, 3(8): 326-21. doi: 10.6026/97320630003326

Van der Bruggen, B. Freundlich Isotherm. In: Drioli, E., Giorno, L. (eds) Encyclopedia of Membranes 2014. Springer, Berlin, Heidelberg. https://doi.org/10.1007/978-3-642-40872-4_254-3

Veningtia A., Harimawan A., Lestari D. 2021. Purification of vitamin E from palm fatty acid distillate through neutralization, extraction, and adsorption methods. IOP Conference Series: Materials Science and Engineering, 1143, 012062. doi:10.1088/1757-899X/1143/1/012062

Wang, X. and Quin P.J. 1999. Vitamin E and its function in membranes. Progress in Lipid Research, 38(4): 309–336. doi:10.1016/s0163-7827(99)00008-9

Xu, H., Lee, U., & Wang, M. 2020. Life-cycle energy use and greenhouse gas emissions of palm fatty acid distillate derived renewable diesel. Renewable and Sustainable Energy Reviews 2020, 134: 110144. doi:10.1016/j.rser.2020.110144

Zhang, QW., Lin, LG. & Ye, WC. 2018. Techniques for extraction and isolation of natural products: a comprehensive review. Chin Med., 13: 20. https://doi.org/10.1186/s13020-018-0177-x